Available online at www.sciencedirect.com
SCIENCE DIRECT
Journal of Photochemistry and Photobiology A: Chemistry 172 (2005) 258–268
Journal of Photochemistry and Photobiology A:Chemistry
www.elsevier.com/locate/jphotochem

Photochemistry of 2′-halobenzanilides: reaction mechanism

Ahmed M. Mayouf*

Laser Research Laboratory, Tajura Research Centre, P.O. Box 84301, Tripoli, Libya

Received 15 April 2004; received in revised form 4 October 2004; accepted 15 December 2004
Available online 27 January 2005

Abstract

The UV photolysis of acetonitrile solutions of 2′-halobenzanilide were followed by UV-spectroscopy, HPLC and time resolved laser flash photolysis. The chemical yields of the major products produced from the irradiation with medium pressure Hg-lamp were measured. The chemical yields of the photosubstitution product ranged from 3 to 45% (the yield was 3% when the starting material was a solution of 2′-chlorobenzanilide in CH_3CN and was 45% when the starting material was a solution of 2′-bromobenzanilide in 10% 1 mol NaOH:CH_3CN). The quantum yield measurements of the photoproducts were carried out in N_2 and O_2 atmosphere in the presence and absence of OH ions. The results showed an enhancement in the yield of the photosubstituted product in the presence of OH ions and in switching from chloro- to bromo-substituent. The presence of O_2 lowered the yield of photosubstitution and photoreduction products. Time resolved studies showed two peaks, one appeared at 395 nm and the second centred around 315 nm. These two peaks were identical in both cases of 2′-halobenzanilides (halo = Cl or Br).

Keywords: Photosubstitution; Photoreduction; 2′-Halobenzanilides

1. Introduction

The photochemistry of aryl halides [1–7] and benzanilides [8–19] has received great attention due to their values of producing several useful compounds. These compounds have interesting applications in different fields; such as medicine, industries, and material sciences [20–23]. Photocyclization is one of the promising methods of producing important cyclic compunds. When aryl halides are photolysed in aromatic solvents; the reaction of the primary photoproduct leads to arylation products. While, when the photoreaction is carried in hydrogen donor solvents reductive dehalogenation, nucleophilic photosubstitution and inter and intramolecular arylation reactions were observed [24,25]. There are two mechanisms suggested for the carbon–halogen bond cleavage. The first mechanism is the homolytic dissociation of the carbon–halogen bond in which the halogen and aryl radicals are formed [1,26,27]. The second mechanism is the electron transfer mechanism in which the electron donor reacts with singlet excited aryl halides to form a radical anion that dissociates to form an aryl radical and a halide ion [28–30]. The dissociation of the carbon–halogen bond may take place either from the higher vibronic energy levels of the lowest excited state [31] or from the higher electronic states that can be populated by photolysis at the absorption maximum of the haloarenes [9,31].

The present investigation on the photoproducts of 2′-halobenzanilide was to elucidate the mechanisms of the formation of these products during the irradiation process using both conventional and time resolving techniques.

2. Materials and methods

2.1. Materials

HPLC grade acetonitrile (J.T. Backer) and triple-distilled water were used all throughout this work. Cyclohexane,

* Present address: NON, NA, 13 Carlton Road, Salford M6 7EW, UK. Tel.: +44 788 1967157.
E-mail address: mais250196@yahoo.com.

1010-6030/$ – see front matter © 2004 Elsevier B.V. All rights reserved.
doi:10.1016/j.jphotochem.2004.12.013

ethylacetate, *n*-hexane, ethanol and methanol (Fisher scientific, HPLC grade) were used. Other chemical reagents such as haloanilines, benzoylchloride, sodium hydroxide and mercuric acetate were analytical grade. They were used without any further treatment.

2.2. Preparation of 2′-halobenzanilide (halo = H, Cl, and Br)

2.2.1. General procedure for the synthesis of 2′-halobenzanilide

The desired 2-haloaniline (0.02 mol) was stirred in 20 ml of pyridine and one equivalent of benzoyl chloride (2.8 g, 0.02 mol) was added drop wise at ice-bath temperature. The mixture was stirred in ice-bath for 2 h and in room temperature for 3 h. When 250 ml of water was added, a white solid was precipitated. The resulting solid was isolated and dried overnight at 55 °C.

2.2.1.1. 2′-Chlorobenzanilide. Yield 66%; mp (crystallised from *n*-hexane) 100–102 °C (lit. value 103.5 °C) [32]; UV (λ_{max} in acetonitrile) 260 nm ($\varepsilon_{260} = 1.2 \times 10^4$ dm^3 mol^{-1} cm^{-1}); IR (KBr) 3225, 3059, 1653 cm^{-1}; ^{1}H NMR (400 MHz, DMSO-D$_6$) δ 10.06 (s, 1H), 8.01 (dt, $J = 6.9$, 1.5 Hz, 2H), 7.60–7.54 (m, 5H), 7.40 (td, $J = 6.0$, 1.6 Hz, 1H), 7.33 (td, $J = 6.0$, 1.5 Hz, 1H); MS *m*/*z* (rel. intensity) 233 (25, M$^+$+2) 231 (93, M$^+$), 196 (15, M$^+$−Cl). Analytical Cal. for $C_{13}H_{10}ONCl$:C, 67.40; H, 4.35; N, 6.05. Found: C, 67.40; H, 4.37; and N, 5.97.

2.2.1.2. 2′-Bromobenzanilide. Yield 97%; mp (crystallised from cyclohexane) 115–117 °C (lit. value 112.5 °C) [32]; UV (λ_{max} in acetonitrile) 259 nm ($\varepsilon_{259} = 8.7 \times 10^3$ dm^3 mol^{-1} cm^{-1}); IR (KBr) 3275, 3055, and 1651 cm^{-1}; ^{1}H NMR (400 MHz, DMSO-D$_6$) δ 10.05 (s, 1H), 8.01 (dt, $J = 6.9$, 1.8 Hz, 2H), 7.72 (dd, $J = 6.9$, 1.2 Hz, 1H), 7.63–7.51 (m, 4H), 7.43 (td, $J = 6.6$, 1.5 Hz, 1H), 7.20 (td, $J = 6.3$, 1.5 Hz, 1H); MS *m*/*z* (rel. intensity) 277 (4, M$^+$+2), 275 (3, M$^+$), 196 (26, M$^+$-Br). Analytical Cal. for $C_{13}H_{10}ONBr$:C, 56.55; H, 3.65; N, 5.07. Found: C, 56.61; H, 3.64; N, 4.99.

2.3. Preparative photoreaction of 2′-halobenzanilide

2.3.1. Photoreaction of 2′-bromobenzanilide

A solution of 2′-bromobenzanilide (0.7 mmol, 0.20 gm) in 500 ml of CH_3CN was photolysed with medium pressure mercury lamp (immersion type-450 W, 110 V) for 1.5 h in N_2 gas at 4 °C. After irradiation, the solution was dried and the residue was dissolved in minimum amount of 1–4 mixture of ethylacetate:*n*-hexane (50 ml). The solution was developed with ethyl acetate:*n*-hexane (1–4) on a preparative TLC (20 cm × 20 cm glass plates, silica gel 60). Six components whose retention factors (R_f-values) were 0.06, 0.11, 0.24, 0.67, 0.73 and 0.78 were seen on the plate. They were identified as phenanthridone (**6**), benzanilide (**3**), 4′-amino-3-bromobenzophenone (**5**), 2′-bromobenzanilide (recovered), 2-phenyl-1,3-benzoxazole (**2**) and 2′-amino-3-bromobenzophenone (**4**), respectively (Scheme 1). Identical photoproducts were also obtained and separated when the solution of 2′-bromobenzanilide was photolysed in 400 ml acetonitrile:100 ml 1 M aqueous NaOH.

2.3.2. Photoreaction of 2′-chlorobenzanilide

When 2′-chlorobenzanilide (1.0 m mole, 0.24 gm) in 500 ml of CH_3CN (or in 400 ml acetonitrile:100 ml 1 M aqueous NaOH) was photolysed with medium pressure mercury lamp for 4.00 h. The same products as with the 2′-bromobenzanilide were separated and identified.

The HPLC analysis of the photoproducts revealed the formation of five analogical major products corresponding to those formed in photolysis of 2′-bromobenzanilide.

The chemical yields from **1b** relative to **1a** demonstrate [33] an increase in the yield of photoreduction and photosubstitution products, while the yield of photofries type products were reduced.

2.4. Relative rate

Each 2.5 ml solution of **1a** (1.25×10^{-4} mol dm^{-3}) or **1b** (1.72×10^{-4} mol dm^{-3}) was photolysed in different conditions (Table 1) for 7 h with 260 ± 9 nm monochromatic light (150 W Xe-lamp). The relative rate of each component was calculated from the ratio of its HPLC peak area in different conditions, relative to its area in acetonitrile/nitrogen.

2.5. Quantum yield

A solution of **1a** (2.5 ml, 1.50×10^{-4} mol dm^{-3}) in acetonitrile purged with nitrogen (or oxygen) for 30 min in 1 cm cuvette was irradiated with 260 ± 7 nm monochromatic light from 150 W Xe-lamp for 4 h. After irradiation, the samples were analyzed by HPLC analytical column (Rainin Microsorb MV C18, 15 cm × 2 mm i.d.). The column was eluted by 25% H_2O:CH_3CN (v/v). In order to calculate the concentration of photoproducts, biphenyl was used as an internal reference. The quantum yields were also calculated for the solution of **1a** in acetonitrile containing 10% by volume of 1 M aqueous NaOH.

Similarly, solutions of **1b** (2.5 ml, 2.0×10^{-4} mol dm^{-3}) were irradiated in the same manner as mentioned above for 2 h and the concentrations of photoproducts were calculated from the HPLC analyses using internal reference. Light intensity was measured by ferroxalate actinometer [34]. The results are presented in Table 2.

2.6. Product distribution

A solution of 2′-bromobenzanilide (0.7 mmol, 0.20 gm) in 500 ml of 10% 1 M aqueous NaOH:CH_3CN was photolysed with medium pressure mercury lamp (immersion type-450 W, 110 V), the irradiation time was 1.5 h and the solution

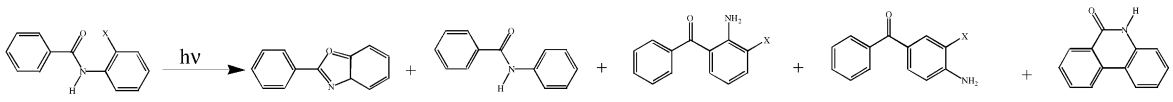

1a: X = Cl
1b: X = Br

2 **3** **4a**: X=Cl **4b**: X=Br **5a**: X=Cl **5b**: X=Br **6**

Scheme 1.

Table 1
Relative rate of the formations of products **2**–**5** in the photoreaction of 2′-halobenzanilides with a monochromatic light from Xe-lamp ($\lambda_{irr} = 260 \pm 7$ nm)

Starting material	Solvent (condition)	Atmosphere	Relative rate			
			2	3	4	5
1a	AN	N_2	1.0	1.0	1.0	1.0
1a	AN	O_2	0.3	0.9	8.1	1.0
1a	AN + NaOH	N_2	2.1	0.5	5.4	0.7
1b	AN	N_2	3.6	3.9	3.3	1.1
1b	AN + NaOH	N_2	8.4	2.3	3.7	0.8

Table 2
Quantum yield of the photoproducts **2**–**5** on the irradiation of 2′-halobenzanilides in different media

Starting material	Solvent (condition)	Atmosphere	Quantum yield × 10^3			
			2	3	4	5
1a	AN	N_2	0.42	0.45	0.11	0.51
1a	AN	O_2	0.13	0.39	0.89	0.52
1a	AN + NaOH	N_2	0.87	0.22	0.59	0.36
1b	AN	N_2	1.53	1.76	0.36	0.57
1b	AN + NaOH	N_2	3.53	1.04	0.41	0.40

was purged with N_2 gas during irradiation. Samples of 1 ml solution were collected every 10 min interval during the photolyses. HPLC were taken for each collected sample and the area of different components were plotted versus irradiation time (Fig. 1). It is obvious that there is no severe effect on the photoproducts. Irradiation time up to 60 min shows a smooth growth of the photoproducts.

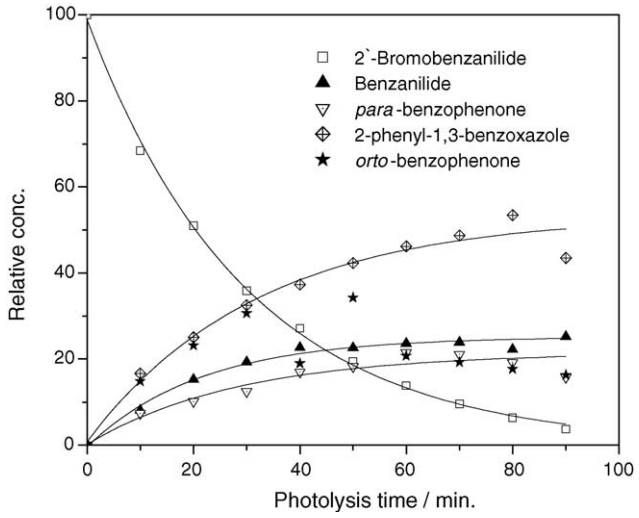

Fig. 1. The product distribution from the irradiation of 2′-bromobenzanilide (1.43×10^{-4} mol dm^{-3}) in 90% acetonitrile, 10% 1 M aqueous sodium hydroxide.

2.7. UV-absorption spectral changes upon irradiation time

A solution of **1a** (2.5 ml, 1.17×10^{-4} mol dm^{-3}) in acetonitrile purged with nitrogen for 30 min was photolysed with Xe-lamp. Cut-off filter of alcohol reagent (90.5% C_2H_5OH, 4.5% CH_3OH, and 5.0% iso-C_3H_7OH by volume) was used to eliminate wavelengths shorter than 215 nm. The change of the UV-spectra against photolysis time is shown in Fig. 2a. The changes of the UV-spectra against photolysis time were also measured for **1a** in a solution of acetonitrile containing 10% of 1 M aqueous NaOH (Fig. 2b). Similarly, the change of the UV-spectrum of **1b** (2.5 ml, 1.43×10^{-4} mol dm^{-3}) is presented in Fig. 2c and d.

2.8. UV-absorption and emission spectra

The absorption spectrum of 2.5 ml of an acetonitrile solution of **1b** (1.2×10^{-4} mol dm^{-3}) in 1-cm quartz cuvette was measured by Jasco 500 UV spectrophotometer. The spectrum showed a λ_{max} at 260 nm (solid line, Fig. 3). Then, a 100 μl of 1 M aqueous NaOH was added and the spectrum recorded again. The spectrum in basic medium showed a structureless

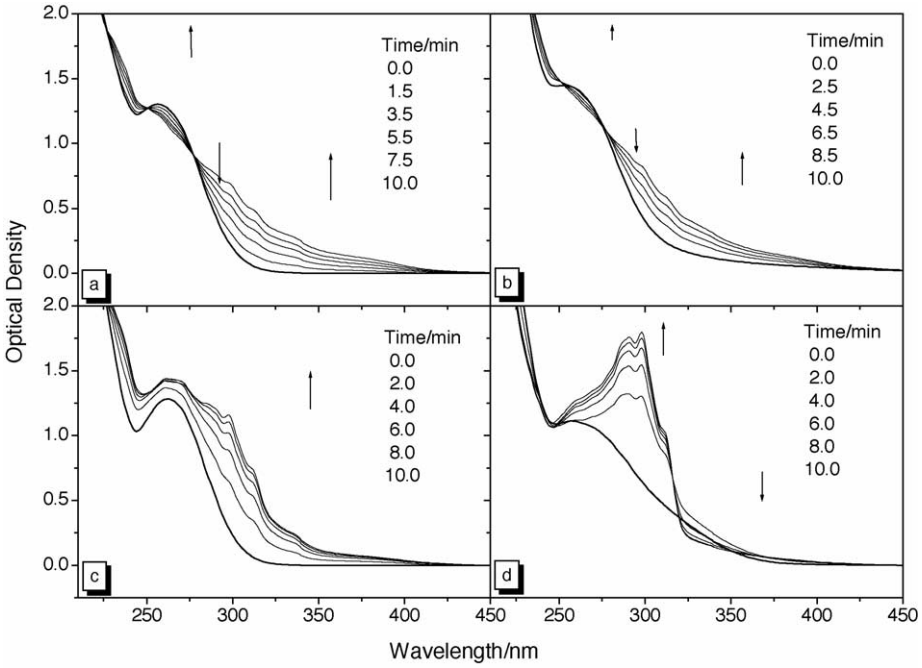

Fig. 2. The change of the UV-spectra of 2′-halobenzanilides with irradiation time. (a) 2′-Chlorobenzanilide (1.17×10^{-4} mol dm^{-3}) in acetonitrile, (b) 2′-chlorobenzanilide (1.17×10^{-4} mol dm^{-3}) in 90% acetonitrile, 10% 1 M aqueous sodium hydroxide, (c) 2′-bromobenzanilide (1.43×10^{-4} mol dm^{-3}) in acetonitrile, and (d) 2′-bromobenzanilide (1.43×10^{-4} mol dm^{-3}) in 90% acetonitrile, 10% 1 M aqueous sodium hydroxide (the thick lines presents the spectra before irradiation).

band extended to 375 nm (dashed line, Fig. 3). When the spectrum, which was measured in neutral solution was subtracted from the one measured in basic medium, a band at 305 nm appeared corresponding to the imidol anion, associated with a negative absorption at 260 nm corresponding to the remaining amide (dotted line, Fig. 3).

The emission spectra of 1.29×10^{-4} mol dm^{-3} solution of 2′-bromobenzanilide were measured in different media

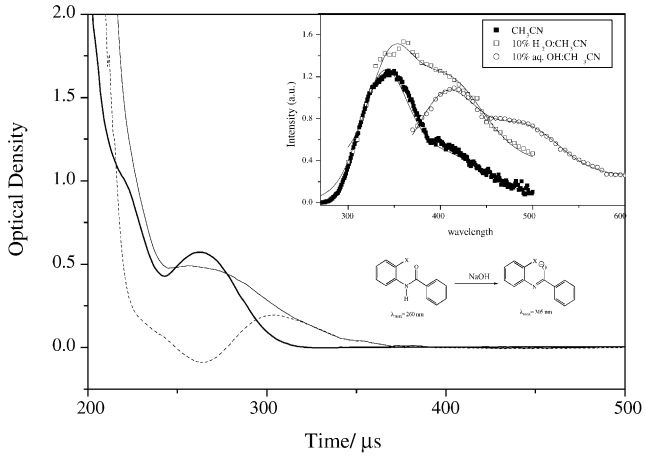

Fig. 3. Absorption spectra of 2′-bromobenzanilide (7.25×10^{-5} mol dm^{-3}). (a) Acetonitrile (solid line) (b) acetonitrile, NaOH (dashed line) and (c) subtraction of the spectrum a from spectrum b (dotted line). Inset: the emission spectra measured in different solvent after 200 ns of the laser pulse.

after 200 ns delay of a laser pulse. The spectra (inset: Fig. 3) showed emission peaks at 344, 400, and 488 nm, respectively.

2.9. Transient absorption and decay profile

About 0.03 g of the starting material **1b** (or **1a**) was dissolved in 1000 ml acetonitrile. The solution was purged with argon and circulated through a flow-type cuvette of 1-cm path length. The time resolved transient spectra (Fig. 4) were measured at different delay times after the laser flash with a boxcar. A similar concentration was used for measuring the decay profile (Figs. 5 and 6) of the observed transients. The time profiles were measured with digital storage oscilloscope (500 MHz).

2.10. Effect of irradiation wavelengths

A 2.5 ml of 1.3×10^{-4} mol dm^{-3} acetonitrile solution of **1a** (or 1.75×10^{-4} mol dm^{-3} of **1b**) was deoxygenated by nitrogen gas (purged 30 min prior to photolysis). The deoxygenated solution was then photolysed with monochromatic light from Xe-lamp for 4.0 h; the photolysis wavelengths were 260 ± 9 and 205 ± 9 nm, respectively. After photolysis, the samples were analysed by HPLC. The ratios of the area of the corresponding peaks were presented in Table 3.

2.11. Instrumentation

Melting points were measured with a Thomas Hoover capillary melting point apparatus. The changes in the

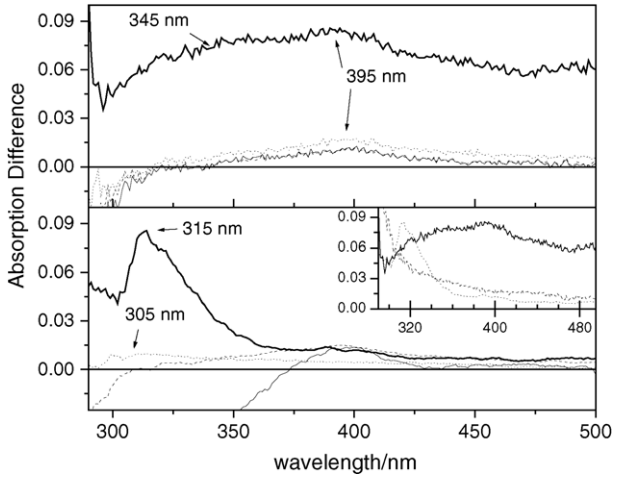

Fig. 4. Time resolved spectra of 2′-bromobenzanilide (1.08×10^{-4} mol dm^{-3}) in acetonitrile (top) and in acetonitrile containing NaOH (bottom): taken after 1 μs (solid thick line), 3 μs (solid thin line), 5 μs (dotted line) and 10 μs (dashed line) after laser pulse. The effect of oxygen on the transient measured at 1 μs after the pulse is shown in the inset (CH_3CN:Ar thick, CH_3CNOH:Ar dashed, and CH_3CNO_2, dotted line).

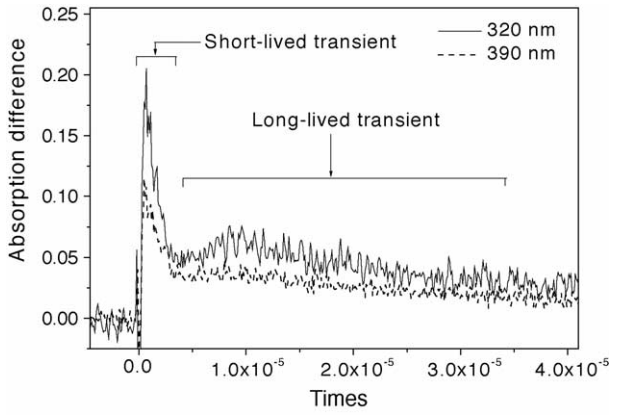

Fig. 5. Time profile of 2′-bromobenzanilide (8.20×10^{-5} mol dm^{-3}) in acetonitrile (time/div. = 5 μs) measured at: 320 nm (solid line) and 390 nm (dotted line).

UV-spectrum of irradiated solution were followed and measured by Jasco 500 spectrophotometer. NMR spectra were recorded by Brucker 400 MHz. Dynamex HPLC chromatography, equipped with Microsorb MV C18 (15 cm × 2 mm i.d.) analytical column was used for the analysis of photoproducts. Elementary analyses were performed on Carlo Erba E.A 1180.

In laser flash photolysis experiments, an excitation source 266 nm was obtained from the third harmonic output of Q-switched Nd:Yag laser (spectron SL803G). The pulse width was ca. 5 ns with typical pulse energy of 55 mJ. The monitor light source (collimated at the right angle of exciting beam) was CW Xe-arc lamp (Atago Bussan co. XC-150). The monitor light was focused through the sample cell into the entrance slit of 320 mm Jabon–Yvon HR320 monochromator. The signals were detected with a Hamamatsu R955 photomultipler tube, amplified by a 300 MHz preamplifier (Stanford Research System SR445). The amplified signal then sampled either by a boxcar signal averger (Stanford Research System SR250) for spectral measurements or digital storage oscilloscope (DSO 500 MHz, Hewlett Packard HP 54503A) for time-decay measurements. A PIN photodiode from Hamamatsu model S1190-13 with a rise time of about 1 ns was used for the triggering of boxcar and DSO. The triggering signal allows for a time resolution down to 10 ns.

The conventional light source was Xe-lamp (450 W). Alcohol reagent cut off filter that eliminates the wavelength shorter than 215 nm was used in 10 mm path length quartz cuvette. Monochromatic light was obtained by using applied photophyiscs monochromator. In case of preparative synthetic reactions, a medium pressure of 450 W Hanova Hg-lamp (immersion type) was used.

Table 3
The effect of the irradiation wavelength on the ratio of the photoproducts

Starting material	[Product] 260/205 nm				
	2	3	4	5	6
1a	21	5.7	0.10	0.02	7.5
1b	14	5.2	0.14	0.25	3.4

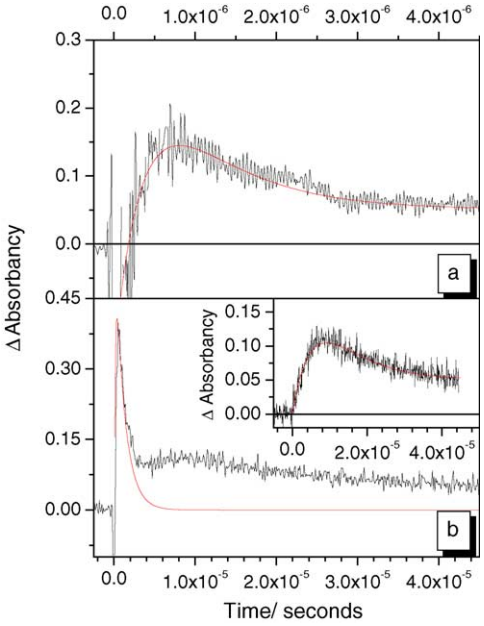

Fig. 6. Time profile of 2′-bromobenzanilide (1.08×10^{-5} mol dm^{-3}) in acetonitrile measured at 390. (a) Time/div. = 0.5 μs, the smooth line is the theoretical fit of the experimental residue. (b) Time/div. = 5.0 μs, the smooth line is the theoretical fit of the experimental residue of the top (inset: the results of the subtraction of the theoretical curve from experimental residue).

3. Results and discussion

3.1. Kinetics

The steady state photoreactions were carried out for the solutions of 2′-halobenzanilides (halo = Cl, Br) either with

Xe-lamp or medium pressure Hg-lamp. In the former case, a cut-off filter of an alcohol reagent in 1-cm cell was used. The changes of the UV-spectra upon irradiation time were followed. The changes in the UV-spectra of **1a** (Fig. 2a) showed sharp isosbestic points at 228, 251, and 278 nm, respectively. These isosbestic points were not altered on going from neutral to the basic media (Fig. 2b), regardless whether the photolysis was carried out in oxygen or nitrogen atmosphere.

When the acetonitrile solution of **1b** was photolysed, the UV-spectral change (Fig. 2c) showed only one isosbestic point at 226 nm and the whole range of the spectrum was increased steadily. In the presence of OH ions (Fig. 2d), the change of the UV-spectra of **1b** showed isosbestic points at 317 and 370 nm. Needless to say that the isosbestic point at 317 nm refers to the formation of phenyl benzoxazole and that at 370 nm refers to the formation of benzophenone. The final spectrum of the irradiated solution of **1b** after ∼10 min photolysis matched exactly the UV-spectrum of 2-phenyl-1,3-benzoxazole.

The relative rates of photochemical reactions of 2′-halobenzanilide are shown in Table 1. The results in the table obviously demonstrate the influence of the living group on the formation rate of photoproducts, as well as the effect of reaction media. For example, the relative rate of formation of benzanilide **3** in presence of NaOH is reduced to half of its value in pure acetonitrile (entries 1 and 3 of column 5, Table 1), while the relative rate of formation of benzoxazole **2** in presence of NaOH is twice of its value in pure acetonitrile (entries 1 and 3 of column 4, Table 1). Similar, the relative rate of **2** produced from **1b** is about four times higher than that produced from **1a** (entries 3 and 5 of column 4, Table 1).

The quantum yield (Table 2) of the formation of 2-phenyl-1,3-benzoxazole **2**, benzanilide **3**, 2-amino-3-X-benzophenone **4** and 4-amino-3-X-benzophenone **5** were determined under different experimental conditions. The quantum yield of products **2** and **3** were 0.424×10^{-3} and 0.452×10^{-3}, respectively in N_2-atmosphere, the corresponding values in presence of oxygen were 0.128×10^{-3} and 0.390×10^{-3}, respectively. The presence of OH ions produced a substantial increase in the yield of the photosubstituted product **2**. The quantum yields of the photosubstituted products formed from irradiation of **1a** were 0.87×10^{-3} and 0.42×10^{-3} in the presence and absence of OH ions, respectively. The corresponding quantum yields from irradiated **1b** were 3.53×10^{-3} and 1.53×10^{-3}, respectively.

The irradiation wavelengths also showed a drastic change in the relative rates of photoproducts (Table 3). The photoreduction yield from **1a** irradiated with 260 nm is 5.7 times to that formed from irradiation with 205 nm, photocyclization being 7.5 times higher, whereas photosubstitution 21 times higher. Meanwhile, the photo-Fries products were about 10–50 times higher with **1a** irradiated with 205 nm relative to 260 nm. The same trend has been observed in irradiation of **1b** (Table 3). These results suggest that the photoreduction, photocyclization and photosubstitution reactions mainly occurred from lower excited states, while the photo-Fries reactions occurred from the higher excited states.

3.2. Laser flash photolysis

The absorption spectrum of **1a** and **1b** in acetonitrile were similar, both compounds showed λ_{max} at 260 nm (ε_{260} of **1a** is 12,000 $dm^3\,mol^{-1}\,cm^{-1}$, and ε_{260} of **1b** is 8700 $dm^3\,mol^{-1}\,cm^{-1}$). Presence of water caused no changes in the absorption spectra, however, in the presence of NaOH the peak intensity was lowered and the spectrum changed to a non-structural band with a long tail extended to 375 nm (Fig. 3). Subtracting the spectrum taken in CH_3CN solution (solid line in Fig. 3) from that one taken in CH_3CN:NaOH solution (dashed line in Fig. 3) resulted in a spectrum consisting of a peak at 305 nm and a negative absorption at 260 nm (dotted line in Fig. 3). The peak at 305 nm can be assigned to the imidol anion form of benzanilide produced by hydrogen abstraction in the presence of strong base.

The emission spectrum of **1a** (inset of Fig. 3) measured in acetonitrile solution (λ_{ext} = 260 nm) consists of a band at 344 and a shoulder at 400 nm with a tail expanded up to ≅550 nm(solid squares). The shoulder at 400 nm became more intensive in the presence of water (open squares). In the presence of NaOH (open circles), two relatively intensive broad fluorescence bands were observed one at 400 nm and the second appeared at 488 nm, the peak at 344 nm being relatively week. Upon further irradiation, the peak at 400 nm decreases and the one at 488 nm increase. It is assumed that, the luminescence peak at 344 nm in acetonitrile arises from the locally excited singlet state (S_1(LE)→S_0) of the keto amide IIA (Scheme 2) and that one at 400 nm arise from the excited state of the imidol anion IIC, respectively. In the basic medium, the luminescence peak centred at 488 nm assumed to originate from the intramolecular electron-transfer excited state that produces the enolate radical anion CTRA. Similar species was observed and reported by park [11] from the irradiation of haloarene.

The acetonitrile solution of **1b** was saturated with argon free oxygen and irradiated by 266 nm laser pulse in 10 mm path length UV-cell (1.00 l reservoir). The spectra obtained at different delay times are presented in the top panel of Fig. 4. The spectrum measured after 1 μs (solid thick line) showed broadband at 395 nm. After 3 μs (solid thin line); the intensity of the band decreased remarkably, then restarted to increase with increasing time.

The aqueous acetonitrile solution of **1b** was saturated with argon free oxygen gas in presence of sodium hydroxide. When the sample was measured after 1 μs, the resulted spectrum (lower panel of Fig. 4) showed a long tail band with a relatively sharp peak at 315 nm. After 3 μs, the peak at 315 nm disappeared and a new peak appeared at 395 nm. The region of the spectrum below ∼370 nm was governed by a strong luminescence. In a relatively longer time (50 μs delay), again

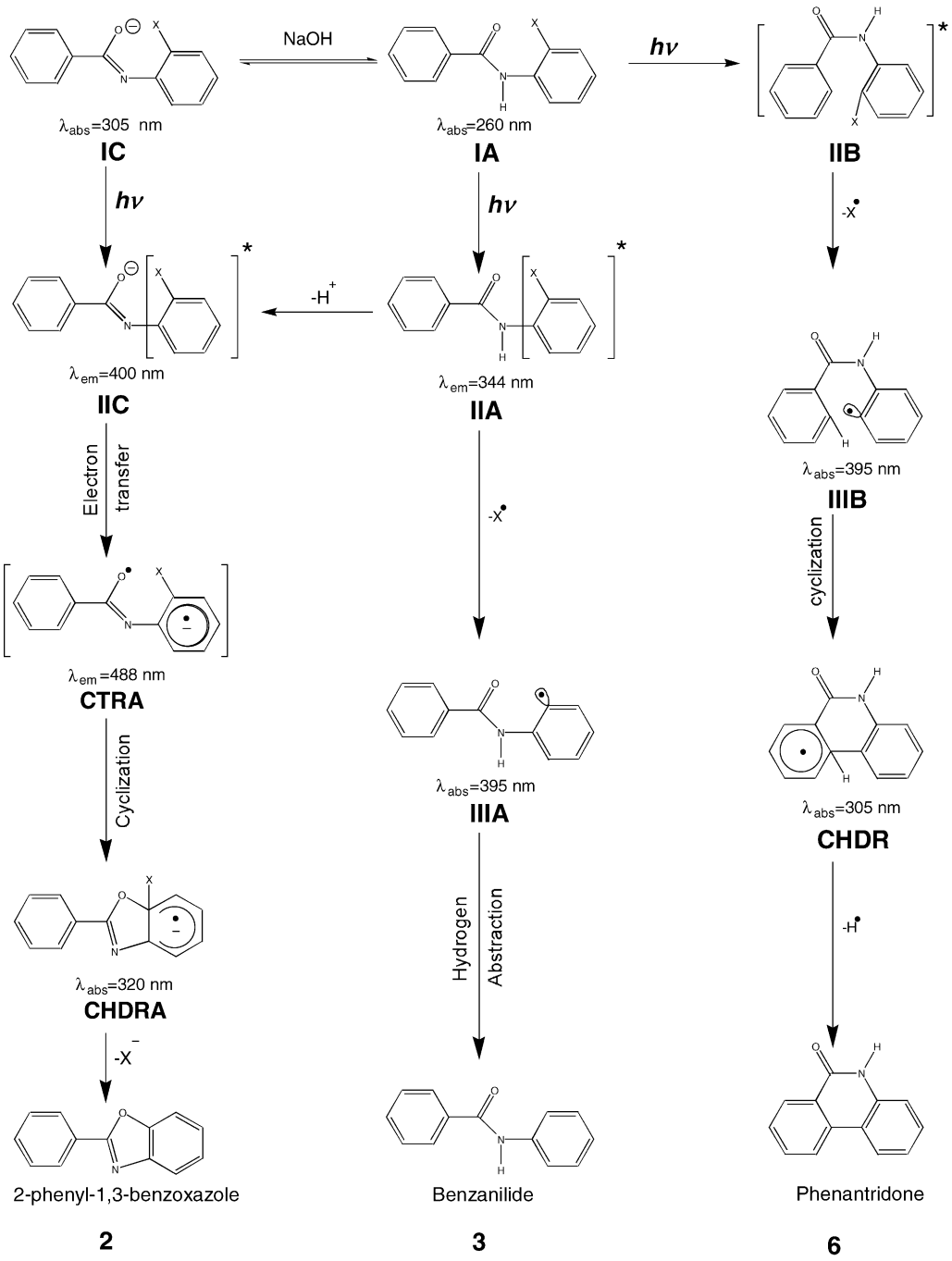

Scheme 2.

a weak signal with a maximum at ∼305 nm and a long tail was observed. The transient spectra of **1a** showed identical feature of the transient spectra of **1b** in terms of time and medium effect.

The decay profiles at different wavelengths showed the same decay pattern (Fig. 5). The profiles consist of an overlapping of more than one transient; one transient formed and decayed in short time and the second transient formed and decayed in relatively longer time. In order to measure the formation and the decay rates of the short-lived transient, one should use a short delay time (0.5 μs/div, Fig. 6a). The formation rate of the short-lived transient, which was measured at 320 nm was $2.71 \times 10^6\ s^{-1}$ when the parent molecule was **1a** and was $5.78 \times 10^6\ s^{-1}$ when the parent molecule was **1b** and its lifetime was ∼1.50 μs regardless of the starting materials.

The formation rate of the short-lived transient, which measured at 390 nm was $4.78 \times 10^6\ s^{-1}$ when the parent molecule

was **1a** and was $5.36 \times 10^6\ s^{-1}$ when the parent molecule was **1b** and its lifetime was ~1.95 μs regardless of the starting materials.

Fig. 6b displayed the time profile measured in 5 μs delay time at 320 nm; the part of the profile that presents the short-lived transient was fitted with two exponential equation by using the formation and decay rate values that are obtained from Fig. 6a, the fitting is presented by the smooth curve shown in Fig. 6b. Subtracting the smooth curve from the experimental residue resolved the time profile of the long-lived transient. The result of the subtraction is shown in the inset of Fig. 6b. The fitting values of these profiles gave the formation rates and the lifetimes of the observed transients as presented in Table 4.

The formation rate of the short-lived transient at 315 nm was $2.73 \times 10^5\ s^{-1}$ and its lifetime was 28.8 μs regardless of the starting materials. The formation rate of the long-lived transient at 395 nm was $3.02 \times 10^5\ s^{-1}$ and its lifetime was 29.33 μs for chloro- and bromo-derivatives. One would expect that the decay rate of the short-lived species measured at 390 nm ($\tau = 1.95$ μs, and $k_d = 5.42 \times 10^5\ s^{-1}$) must match the formation rate of the long-lived transient at 320 nm ($k_f = 2.73 \times 10^5\ s^{-1}$), but because of the potential interference of the absorptions of short-lived and long-lived transients at measured wavelengths, these values were different. Recalculating the decay rate of the long-lived transient at 300 nm instead of 320 nm gives better inference, in which the decay rate was $5.25 \times 10^5\ s^{-1}$.

3.3. Reaction mechanisms

The photolysis of 2′-halobenzanilide yielded photocyclization, photoreduction, photosubstitution and *ortho*- and *para*-photo-Fries products. Scheme 2 presents the reaction mechanism based on the photoproduct analysis and the time resolved studies.

The ground state absorption spectra of benzanilide were not affected by the halo-substituent at the *ortho*-position of the anilino ring, the maximum absorption being at about 260 nm (solid line, Fig. 3). In the presence of OH ions, the keto form of the amide IA is in equilibrium with the imidol anion, the maximum absorption of the imidol anion IC being at $\lambda_{max} = 305$ nm (dotted line, Fig. 3).

From the absorption and the emission spectra of halobenzanilide (Fig. 3), the energy of the first excited state of the amide-form was found to be 413 kJ mol^{-1} and the energy of the first excited state of the imidol anion was 354 kJ mol^{-1}. Excitation at 260 nm (476 kJ mol^{-1}) can bring the excited molecules to higher vibronic levels of the first excited state where the homolytic photodissociation of carbon–halogen bonds can be achieved, as well as to the higher excited states.

Homolysis cleavage from the higher excited state (S_2) could also take place, but probably will be competed by the photo-Fries rearrangement process (see the effect of wavelength). Benzanilide, phenanthridone, and benzoxazole yielded from the photolysis of halobenzanilide with 205 nm (shorter wavelength) were quite less than that formed by photolysis with 260 nm (Table 3). Meanwhile, the photo-Fries type products showed an opposite trend, in which their yields were higher when the sample was irradiated with a shorter wavelength compared to that formed by irradiation with a longer wavelength (Table 3). Acetone used as a sensitizer failed to enhance the photoreactions. On the other hand, oxygen has influenced the quantum yield of photoreduction product and photosubstitution product. The transients appeared in the time resolved spectra after 1 μs delay was quenched totally in the presence of oxygen (inset of Fig. 4, bottom panel).

Table 4
The lifetime and the rate of formation of detected transients

Transient	λ_{max} (nm)	Starting material	τ (μs)	Formation rate (s^{-1})
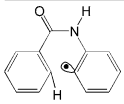 phenyl σ- radical I	395	**1a** **1b**	1.95 ± 0.49	$(4.78 \pm 0.47) \times 10^6$ $(5.36 \pm 0.21) \times 10^6$
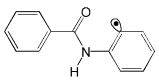 phenyl σ- radical II	395	**1a**, **1b**	29.33 ± 0.32	$(3.02 \pm 0.55) \times 10^5$
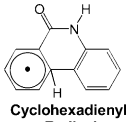 Cyclohexadienyl Radical	305	**1a**, **1b**	28.80 ± 6.59	$(5.25 \pm 0.75) \times 10^5$
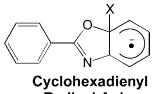 Cyclohexadienyl Radical Anion	315	**1a** **1b**	1.50 ± 0.21	$(2.71 \pm 0.68) \times 10^6$ $(5.78 \pm 1.30) \times 10^6$

Benzanilide **3** and phenanthridone **6** were more likely to be formed through a radical route, which formed from the homolytic cleavage of the carbon–halogen bond, followed by hydrogen abstraction from the solvent molecules in the former case and electrocyclization in the later.

There seems to be no competition between intramolecular photoelectrocyclization and photoreduction processes, since these two products originated from two different states, in which the former is produced from homolytic dissociation of twisted excited species and benzanilide from halogen cleavage in locally excited state. However, the twisted radical also can react with a solvent to produce benzanilide, but the rate of cyclization is much faster than the rate of hydrogen abstraction. Generally, the yield of the photoreduction and electrocyclization is controlled by the conformational ratio of *Z*- to *E*-conformer in excited states. *Z*-conformer preferred a hydrogen abstraction from the solvent to produce a reduction product, while the *E*-conformer would accommodate a molecule to proceed into ring closure and to form phenanthridone **6**. The conformational change has occurred in the $S_1(\pi,\pi^*)$ as well as from higher excited states, in which the rotational barrier about C–N bond reduced [10].

The ring photoclosure of *ortho*-substituted haloarenes was reported for various compounds [1–3,7,8,11,18], 2-halobenzanilide irradiated in deoxygenated cyclohexane [8] gave the corresponding phenanthridone in a yield exceeding 70%. In high concentration solution, a hydrogen-bonded dimer is suggested to form [12,15] and in the excited state this dimer holds the *E*-conformation. Solvents and substituents alter the ratio of these two conformations; the effect is reflected on their yields [8,35,36]. Polar solvents strengthen the amide-bond order and increase the rotational barrier [36,37]; therefore, the conformation IIA became predominant. In less polar solvents and in hydrocarbon solvents, the conformation IIB is more favourable and therefore, the electrocyclization yield is higher than photoreduction [8,18,36]. Blocking the amide resonance by replacing amide hydrogen with methyl group [8,11], or restricting the conformational change through a complexation [9,18] leads to a high yield of photocyclization relative to photoreduction.

Another example of ring closure in photochemistry of *ortho*-substituted haloarenes is the intramolecular photosubstitution reaction in which the halogen of excited haloarenes is substituted by nucleophile [4,11,38–42]. According to this mechanism, the electron-transfer from the carbonyl or thio group of excited molecule to deficient halo-arene ring assists the heterocleavage of halogen–carbon bond.

In the case under the study, the electron-transfer from the carbonyl group of excited imidol anion IIC to deficient anilino ring assists the heterolytic cleavage of halogen–carbon bond. The electron-transfer leads to the formation of charge transfer excited state radical anion species (CTRA) that emits at 488 nm. Once CTRA is formed, it proceeds to cyclization to form cyclohexadienyl radical anion CHDRA.

According to the results shown in the previous sections, the lifetime of the short-lived transient at 320 nm was similar in the presence and absence of any quencher (about 1.5 μs), but its intensity was reduced in the presence of oxygen and enhanced in presence of NaOH. Its formation rate was also different when the parent molecules were different. The quantum yields (Table 2) showed a reduction in the formation of the photosubstituted product in the presence of oxygen. The short-lived transient at 320 nm band was assigned to the cyclohexadienyl radical anion CHDRA, the cyclization may be affected slightly by the halogen substituent as it is reflected on the rate of formation, which was $5.78 \times 10^6\ s^{-1}$ when the halogen-substituent was bromo and was $2.71 \times 10^6\ s^{-1}$ when the halogen was chloro-analogue. The ring closure takes place in a relatively short time followed by heterolytic dissociation to form compound **2** and halogen anion.

In basic media, the yield of the photosubstitution product was increased, the intensity of the short-lived transient at 320 nm was also increased (compare Fig. 4 top/bottom panels), but its lifetime remained the same. Therefore, the CTRA would expect to be formed by a path involving excitation of imidol form of benzanilide IC. The excited imidol IIC will lead to the formation of CTRA through an electron transfer.

Meanwhile, the longer-lived species buried under 320 nm was assigned to the cyclohexadienyl radical CHDR. A similar transient was reported [43] in the literature for the reaction of hydroxyl radical or azide radical with multifunctional hetercyclic molecules, the reaction is belived to lead to the formation of cyclohexadienyl radical, its maximum absorption is found at 300 nm. Also, when hydrogen atoms [44], hydroxyl radicals [45] or chloride radicals [46] are added to aromatic benzene, the reactions results in the formation of cyclohexadienyl radical transients. The absorption spectra of the transients were reported in the range of 270–340 nm and the absorption maximum were found at 305 nm.

The band, which appeared in the spectrum (Fig. 3) at 345 nm, can be assigned to the dihalide radical anion $X_2^{\bullet -}$. This radical anion is believed to be produced from the reaction of halogen radical that formed from the homolytic cleavage of carbon–halogen bond of parent compound and the halogen anion that formed from heterloytic cleavage of the carbon–halogen bond of cyclohexadinayl radical anion. So, the presence of $X_2^{\bullet -}$ species is an evidence for homolytic and heterolytic dissociation of carbon–halogen bond of halobenzanilide and hence is an evidence for the formation of its counter phenyl σ-radical and cyclohexadinayl radical anion. The 395-nm band was assigned to the phenyl σ-radical that was produced from halogen cleavage of both the twisted benzanilide in higher excited state IIIB (short-lived transient) and the locally excited benzanilide IIIA (long-lived transient). Dihalide radical anion $X_2^{\bullet -}$ was reported [47] to have an absorption maximum at 340 nm. Jayanthi [48] in his study on the photolysis of chloroacetanilide and Park [11] in the photolysis of haloarenes have reported the observation of $Cl_2^{\bullet -}$ around 350 nm.

Photo-Fries products are formed from the intramolecular rearrangement of the photolysed molecule. The reaction paths involve either the free radical reaction [49,50] and/or a

concerted reaction [50]. The mechanism of photo-Fries products was reported for aryl esters [51,52], in which *ortho*- and *para*-acylphenols were produced from the irradiation of phenyl esters, while acetanilide [49,50] typically gave *ortho*- and *para*-acetylaniline. Many carboxylic acid derivatives [51] under UV photolysis proceed to form photo-Fries products. The photo-Fries mechanism is generally considered as an intramolecular process, in which an α-cleavage of heteroatoms bond in the singlet excited state is followed by in-cage recombination of the radicals. Mainly, the photo-Fries rearrangement takes place at *ortho*- or *para*-position, except in few cases where meta photo-Fries have been reported [53]. In very few examples, radical reactions out of the cage were observed [54], for example, the irradiation of phenyl acetate produced phenoxy radical; the phenoxy radical that escaped from the cage can form a phenol [54]. Photolysis of phenylacetate in the vapour phase produced no photo-Fries products. Formations of phenols in irradiation of phenylacetate in solution and disappearance of photo-Fries products in vapour phase supported the α-cleavage of heteroatoms bond dissociation mechanisms. In another example, the photolysis of *N*,*N*-dimethylbenzamide [55] in the presence of 1,1-diphenylethylene, showed formation of adduct due to the addition of benzoyl radical.

Photo-Fries arrangement [56] suggested occurring from two different excited states of the parent molecule. The higher energy excited state leads to amide bond dissociation and the lower excited state would form rearranged products by a concerted continuously bonded process.

In the photolysis of halobenzanilide, the cleavage of the amide bond leads to the formation of benzoyl radicals and 2-haloanilino radicals. The benzoyl radical recombined with the anilino at *ortho*- and *para*-position to form benzophenone derivatives (**4** and **5**). In the concerted reaction, the electron-rich carbon of carbonyl group interacts with deficient aniline ring at *ortho*-position and/or at *para*-position. Weakening of the nitrogen-ring bond and tightening the carbonyl–carbon to the aniline ring follow this. Thus the *ortho*- and *para*-photo-Fries products **4** and **5** are formed, respectively.

The presence of aromatic ring is supposed to stabilize the formed radicals and hence the out-cage reaction must be expected for these types of radicals. Within the limitation of our experiment, we did not detect any products, which could be attributed to the out-cage reactions, therefore, we assumed that the photo-Fries rearrangement takes place from the lowest singlet exited halobenzanilide according to the concerted mechanism. Contrary to that, the chemical yield of photo-Fries products in the photolysis of benzanilide with short wavelength was found to be several folds higher than those produced by photolysis with longer wavelength. This suggests the formation of photo-Fries products from higher electronic state by amide dissociation mechanism. This implies that both mechanisms were operated in the formation of photo-Fries products.

In conclusion, the reaction mechanism of the halobenzanilides is a bit complicated, due to the formation of many photoproducts in one hand and on the other hand due to the intensive interference of the transient species. The irradiation time used for quantum yield measurements were quite long, but if we consider the results of the product distribution shown in Fig. 1, where the irradiation source was non-chromatic light, the results for the quantum yield can be accepted as the proper results for the photoproducts.

The study represented here highlights the possible mechanism, but there is a strong belief for the need of further studies that involves the careful chosing of the leaving halogen group, the substituent at *para*-position of both rings, the solvent and the wavelength effects in the photoproduct and transient formation.

Acknowledgment

This work was supported by the brain Korea 21 project and Korea basic science institute. The author thanks Prof. Young Tae Park of Department of Chemistry, Kyungpook National University for stimulated discussion.

References

[1] J. Grimshaw, P. de Silva, J. Chem. Soc. Rev. 10 (1981) 181.
[2] Y.-T. Park, C.-H. Joo, C.-D. Choi, K.-S. Park, J. Heterocycl. Chem. 28 (1991) 1083.
[3] Y.-T. Park, N.W. Song, Y.-H. Kim, C.-G. Hwang, S.K. Kim, D. Kim, J. Am. Chem. Soc. 118 (1996) 11399.
[4] R. Arad-Yellin, B.S. Green, K.A. Muszkat, J. Org. Chem. 48 (1983) 2578.
[5] J.F. Wolfe, M.C. Sleevi, R.R. Goehring, J. Am. Chem. Soc. 102 (1980) 3646.
[6] J.R. Lenz, J. Org. Chem. 39 (1974) 2839.
[7] Y.-T. Park, N.W. Song, C.-G. Hwang, K.-W. Kim, D. Kim, J. Am. Chem. Soc. 119 (1997) 10677.
[8] J. Grimshaw, P. de Silva, J. Chem. Soc., Trans. II (1982) 857.
[9] J. Grimshaw, P. de Silva, J. Chem. Soc. Perkin II (1981) 1010.
[10] F.D. Lewis, T.M. Long, J. Phys. Chem. 102 (1998) 5327.
[11] Y.-T. Park, C.-H. Jung, K.-W. Kim, H.S. Kim, J. Org. Chem. 64 (1999) 8546.
[12] G.-Q. Tang, J. Maclnnic, M. Kasha, J. Am. Chem. Soc. 109 (1987) 2531.
[13] D.P. Bandyopadhyay, D. Majumdar, S. Battacharyya, K. Das, J. Molecul. Struct. 367 (1996) 127.
[14] J. Heldt, D. Gormin, M. Kasha, J. Am. Chem. Soc. 110 (1988) 8255.
[15] J. Heldt, J.R. Heldt, J. Kaminski, Z. Naturforsch 54A (1999) 492.
[16] J. Heldt, M. Kasah, J. Mol. Liquids 41 (1989) 305.
[17] J. Heldt, J.R. Heldt, E. Szatan, J. Photochem. Photobiol. A: Chem. 121 (1999) 91.
[18] J. Grimshaw, P. de Silva, Can. J. Chem. 58 (1980) 1880.
[19] I. Azumaya, H. Kagechika, K. Yamaguchi, K. Shudo, Tetrahedron 51 (1995) 5277.
[20] R.J. Lewis, P. Cemellori, A.J. Kirby, C.A. Marby, A. Slawin, D. Williams, J. Chem. Soc., PT II (1991) 1625.
[21] S. Lucht, J. Stumpe, J. Lumin. 91 (2000) 203.
[22] B. Despax, N. Paillous, A. Lattes, J. Appl. Poly. Sci. 27 (1982) 225.
[23] J. Carlos del Valle, M. Kasha, J. Catalan, J. Phys. Chem. 101 (1997) 3260.
[24] N.J. Bunce, J. Bergsma, M.D. Bergsma, W. De Graaf, Y. Kumar, L. Ravanal, J. Org. Chem. 45 (1980) 3708.

[25] J. Siegman, J. Houser, J. Org. Chem. 47 (1982) 2773.
[26] P.G. Sammes, in: S. Patai (Ed.), Chemistry of C–X, Wiley Interscience, 1973, chapter 11.
[27] D.R. Arnold, P.C. Wong, J. Am. Chem. Soc. 99 (1977) 3363.
[28] R. Davidson, J. Goodin, Tetrah. Lett. 22 (1981) 163.
[29] N. Bunce, S. Safe, L.O. Ruzo, J. Chem. Soc. Perkin I (1975) 1607.
[30] J.F. Bunnett, Tetrahedron 49 (1993) 4477.
[31] N.J. Turro, V. Ramamurthy, W. Cherry, W. Farneth, Chem. Rev. 78 (1977) 125.
[32] H.W. Grimmel, A. Guenther, J.F. Morgan, J. Am. Chem. Soc. 68 (1946) 539.
[33] A.M. Mayouf, Y.-T. Park, J. Photosci. 7 (2000) 5.
[34] J.G. Galvert, J.N. Pitts, Photochemistry, Johan Willey, NY, 1966.
[35] D.H. Hey, G.H. Jones, M.J. Perkins, J. Chem. Soc. Perkin I (1972) 1155.
[36] A.M. Mayouf, Y.-T. Park, J. Photochem. Photobiol. A: Chem. 150 (2002) 115.
[37] T. Yuzuri, H. Suezawa, M. Hirota, Bull. Chem. Soc. Jpn. 67 (1994) 1664.
[38] W.R. Bowman, H. Heaney, P.H. Smith, Tetrah. Lett. 23 (1982) 5093.
[39] J.F. Bunnett, B.F. Hrutfiord, J. Am. Chem. Soc. 83 (1961) 1691.
[40] M.F. Semmelhack, T. Barger, J. Am. Chem. Soc. 102 (1980) 7765.
[41] J. Cornelisse, E. Havinga, Chem. Rev. 75 (1975) 353.
[42] P. Kutschy, M. Suchy, A. Andreani, M. Dzurilla, V. Kováčik, J. Alföldi, M. Rossi, M. Gramatova, Tetrahedron 58 (2002) 9029.
[43] O. Brede, J. Schwinn, Leistner, S. Naumov, H. Sprinz, J. Phy. Chem. A 105 (2001) 119.
[44] F. Berho, M.-T. Rayer, R. Lesclaux, J. Phys. Chem. 103 (1999) 5501.
[45] E. Bjergbakkle, A. Sillesen, P. Pagsberg, J. Phys. Chem. 100 (1996) 5729.
[46] O. Sokolov, M. Hurley, T. Wallington, E. Kaiser, J. Platz, O. Nielsen, F. Becho, M.-T. Rayer, R. Lesclaux, J. Phys. Chem. 102 (1998) 10671.
[47] G.V. Buxton, M. Bydder, G.A. Salmon, J. Chem. Soc., Faraday Trans. 94 (5) (1998) 653.
[48] G. Jayanthi, S. Muthusamy, R. Paramasivam, V.T. Ramakrishnan, N.K. Ramasamy, P. Ramamurthy, J. Org. Chem. 62 (1997) 5766.
[49] Y.-T. Park, H.-C. Yun, S.-R. Do, Y.-D. Kim, J. Kor. Chem. Soc. 29 (1985) 441.
[50] D.J. Carlsson, L.H. Gan, D.M. Wiles, Can. J. Chem. 53 (1975) 2337.
[51] J.D. Coyle, Chem. Rev. 78 (1978) 97.
[52] D. Bellus, Adv. Photochem. 8 (1971) 109.
[53] D.R. Crump, R.W. Franck, R. Gruska, A. Ozorio, M. Pagnotta, G. Siuta, J. White, J. Org. Chem. 42 (1977) 105.
[54] C.E. Kalmus, D.M. Herecules, J. Am. Chem. Soc. 96 (1974) 449.
[55] Y. Katsuhara, R. Tsujii, K. Hara, Y. Shigemistu, Y. Odaira, Tetrah. Lett. (1974) 453.
[56] H. Zimmerman, A. Parent, J. Am. Chem. Soc. 92 (1970) 6259.